Clinical Radiology 79 (2024) e665–e674

Contents lists available at ScienceDirect

Clinical Radiology

journal homepage: www.clinicalradiologyonline.net

Quantifying the calcification of abdominal aorta and major side branches with deep learning

J. Halkoaho [a,b,*,†], O. Niiranen [c,d,†], E. Salli [a], T. Kaseva [a], S. Savolainen [a,b], M. Kangasniemi [a], H. Hakovirta [c,e,f]

[a] *Department of Radiology, HUS Diagnostic Center, Helsinki University Hospital and University of Helsinki, Helsinki, Finland*
[b] *Department of Physics, University of Helsinki, P.O. Box 64, FI-00014 Helsinki, Finland*
[c] *Department of Surgery, University of Turku, Turku, Finland*
[d] *Department of Surgery, Seinäjoki Central Hospital, Seinäjoki, Finland*
[e] *Division of Gastroenterology and Urology, Turku University Hospital, Turku, Finland*
[f] *Department of Surgery, Satasairaala, Pori, Finland*

ARTICLE INFORMATION

Article history:
Received 14 July 2023
Received in revised form
20 December 2023
Accepted 17 January 2024

AIM: To explore the possibility of a neural network-based method for quantifying calcifications of the abdominal aorta and its branches.

MATERIALS AND METHODS: In total, 58 computed tomography (CT) angiography volumes were selected from a dataset of 609 to represent different stages of sclerosis. The ground truth segmentations of the abdominal aorta, coeliac trunk, superior mesenteric artery, renal arteries, common iliac arteries, and their calcifications were delineated manually. Two V-Net ensemble models were trained, one for segmenting arteries of interest and another for calcifications. The branches of interest were shortened algorithmically. The volumes of calcification were then evaluated from the arteries of interest.

RESULTS: The results indicate that automatic detection is possible with a high correlation to the ground truth. The scores for the ensemble calcification model were dice score of 0.69 and volumetric similarity (VS) of 0.80 and for the arteries of interest segmentations: aorta: dice 0.96, VS 0.98; aortic branches: dice 0.74, VS 0.87; and common iliac arteries: dice 0.72, VS 0.91.

CONCLUSIONS: The presented neural network model is the first to be capable of automatically segmenting, in addition to calcification, both the aorta and its branches from contrast-enhanced CT angiography. This technology shows promise in addressing limitations inherent in earlier methods that relied solely on plain CT.

Introduction

Cardiovascular diseases are the leading cause of death in the world.[1] They represent a significant global health challenge and impose a considerable burden on healthcare systems and economies. The most prevalent presentations of cardiovascular disease are ischaemic heart disease, cerebrovascular disease, and peripheral arterial disease. Aortic

* Guarantor and correspondent: J. Halkoaho, Department of Radiology, HUS Diagnostic Center, Helsinki University Hospital and University of Helsinki, Vallikallionkuja 5 A 7, Espoo 02650, Helsinki, Finland.
E-mail address: Johannes.halkoaho@helsinki.fi (J. Halkoaho).
† These authors contributed equally to the study.

https://doi.org/10.1016/j.crad.2024.01.023

calcification has been established as a significant predictor of cardiovascular morbidity and mortality. Calcification of the abdominal aorta is associated with poor outcomes in other severe conditions, such as chronic kidney disease, cancer mortality, strokes, and complications in gastrointestinal surgery.[2–10] At present, there are several widely utilised risk scores for cardiovascular risk assessment including Framingham risk score (FRS), SCORE risk chart, American College of Cardiology/American Heart Association (ACC/AHA) risk calculator and QRISK, none of which incorporate aortic calcification as a risk factor.[11–14]

Most methods of quantifying aortic calcification require manual assessment of radiographs or computed tomography (CT) images or the use of thresholding methods, which are challenging to apply to contrast-enhanced imaging.[2,9,15–17] There is also a lack of standardised, objective, reproducible protocols for the assessment of atherosclerotic burden at defined vascular segments leading to heterogeneity in reported methods. Therefore, the comparability of investigations and results is limited.

These limitations have prompted the development of more efficient and reliable techniques that can be applied to large datasets.

One of these techniques is the use of neural network-based methods. In recent years, neural network-based applications have been developed to quantify aortic calcification using both radiographs and unenhanced CT images.[18,19] To the authors' knowledge, no neural network-based methods or other image analysis techniques have been reported as available to automatically quantify aortic calcification from contrast-enhanced CT, which offer improved visualisation of visceral and renal arteries. The aim of present study was to minimise the interobserver variability and to gain an automatic objective and reproduceable score for burden of atherosclerosis at defined arteries. The aim of the present study was to develop a method for analysing the abdominal aorta and its major branches.

Materials and methods

The present sample consisted of patients with peripheral artery disease. All patients underwent CT angiography (CTA) imaging (between 2011–2013) which were performed using standard protocols for CTA at the Department of Radiology, Helsinki University Hospital. Patient files were followed-up until 1 January 2020, which was considered to be the end of the study. The institutional review board of University of Turku reviewed and accepted the study (IRB no. T344/2017). Due to the nature of the study, no informed consent from patients was required. From 609 CTA volumes a total of 58 volumes were selected. Based on previous experience, the number of volumes needed for model training was estimated to be between 50 to 60. Patients in the original sample were assigned a randomised ID number. In order to have a representative sample, the volumes were categorised visually in three groups based on the level of calcification (minimal, moderate and extensive) following the order of the cumulative ID numbers until a suitable-sized training set was identified. From the selected volumes, one volume was excluded due to suboptimal contrast concentration, and another due to being the sole representative of Leriche syndrome in the cohort, resulting in insufficient data for training the model for this condition. The rest of the volumes were divided into the training set (n=41) and the test set (n=15). The diagram of this process is shown in Fig 1. The common parameters are found in Table 1. Manufacturers were GE Medical Systems (for models LightSpeed16; eight in total, three in the test set), Optima CT660 (19 in total, four in the test set), Siemens (for models Sensation 64 (16 in total, three in test set), SOMATOM Definition AS+ (10 in total, four in the test set), and Toshiba (for model Aquilion ONE; three in total, one in the test set). The entire method is illustrated in the flow chart shown in Fig 2.

Ground truth segmentation

Ground truths for each volume of the dataset were created using three-dimensional (3D) Slicer version 5.2.1[20] and a previously developed 2D V-Net.[21] The aorta was first segmented using the two-dimensional (2D) V-Net. The iliac arteries were segmented manually using 3D Slicer up to the iliac bifurcation, while the coeliac artery, superior mesenteric artery, renal arteries, and their respective branches were segmented as individual segments, as far as they could be reliably identified.

Dense plaques with a radiodensity measurement >300 HU were identified and considered as calcifications where anatomically suitable. Intraluminal stents were segmented separately from calcifications where possible. The segmentation task was performed by a vascular surgery resident with 4 years of post-medical school graduation training with guidance and consultation from a senior radiologist with >20 years of experience.

Training of the segmentation models

Two neural network ensemble models comprising five V-Nets[22] with similar architectures as proposed in 21 were trained for two purposes using MONAI framework.[23] The first objective was to concurrently perform segmentation of the abdominal aorta and its visceral and renal arterial branches, as well as the common iliac arteries. The second objective was to segment the calcifications from the relevant vessels. Each neural network used V-Net architecture with the same specifications as proposed in 21, but with the number of filters starting from 8. Each V-Net had a unique training dataset split into 31 volumes used for training and 10 for validation. Data pre-processing during training of all V-Nets was otherwise the same as discussed in 21, but the intensities were scaled to [0,1] interval using −500 and 3,000 intensity cut-offs, training volumes resampled to $1 \times 1 \times 1$ mm spacings for four V-Nets and $1 \times 1 \times 2$mm for the fifth V-Net due to GPU memory constraints and input patch size set to $320 \times 320 \times 64$. During each training, the optimiser was Adam with learning rate 0.001, which was

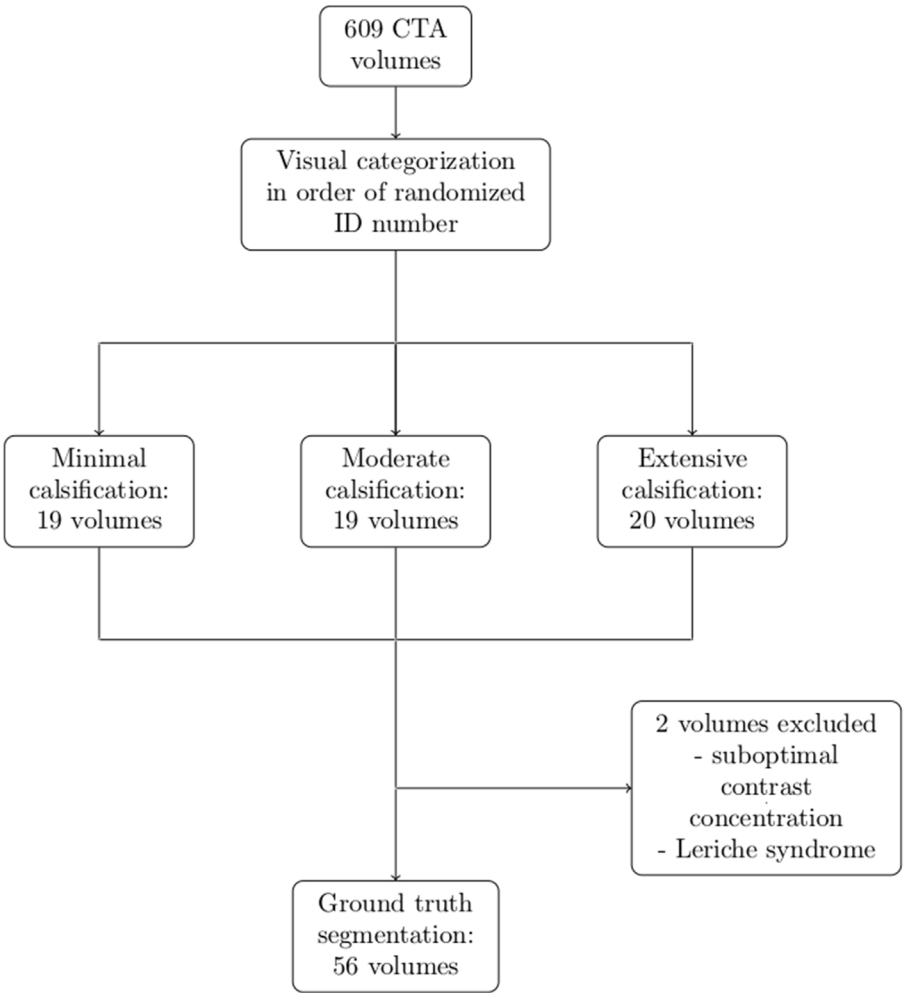

Figure 1 Flowchart demonstrating the selection process of the training set. Volumes were given a cumulative randomised ID number and categorised visually into three groups based on the level of calcification until a suitable-sized training set was identified.

halved after 1,200 steps and loss function combination of multiclass Dice loss and cross entropy loss. The trained V-Net ensemble was used for segmenting the test set of 15 volumes using majority voting. The GPU used was a Tesla v100 32 GB.

Blood vessel segmentation

The arteries were classified into three categories: the abdominal aorta, the common iliac arteries, and the branches of the abdominal aorta, which encompassed the renal arteries, coeliac trunk, and superior mesenteric artery. The V-Nets of the model were trained for an average of 1,760 epochs. Visualisation of an example prediction of the model is illustrated in Fig 2.

Initial artery segmentations, excluding the aorta, were shortened algorithmically to the first 1.5 cm (branches) and 2 cm (common iliac arteries) to represent the proximity of these major abdominal aortic branches. First, utilising SimpleITK v. 2.2.1,[24] a binary label map of the aorta was created and resampled to be isotropic using nearest neighbour interpolator with spacing of the largest dimension of the volume. Then, the aorta was dilated using a ball with a radius of one as a structuring element[25] and then masking it with a binary label map containing either both the aorta and the branches or the aorta and the common iliac arteries. This was repeated until the desired length was achieved. Fig. 3 illustrates the end result.

Table 1
Common parameters of the dataset.

Parameter	Test set (n=15)	Training set (n=41)
Age in years	72 (58–89)	70 (53–90)
Tube voltage range (kV)	80–120	80–120
Gender	10 M, 5 F	26 M, 15 F
Section thickness (mm)	1.8 (1–2.5)	1.9 (1–2.5)
Spacings (mm)	0.84 (0.68–0.98)	0.83 (0.63–0.98)

The average is given for slice thickness, spacings and age with the range in brackets.

Calcification segmentation

The model for segmenting the calcification was trained using two labels: one for all blood vessels and another for

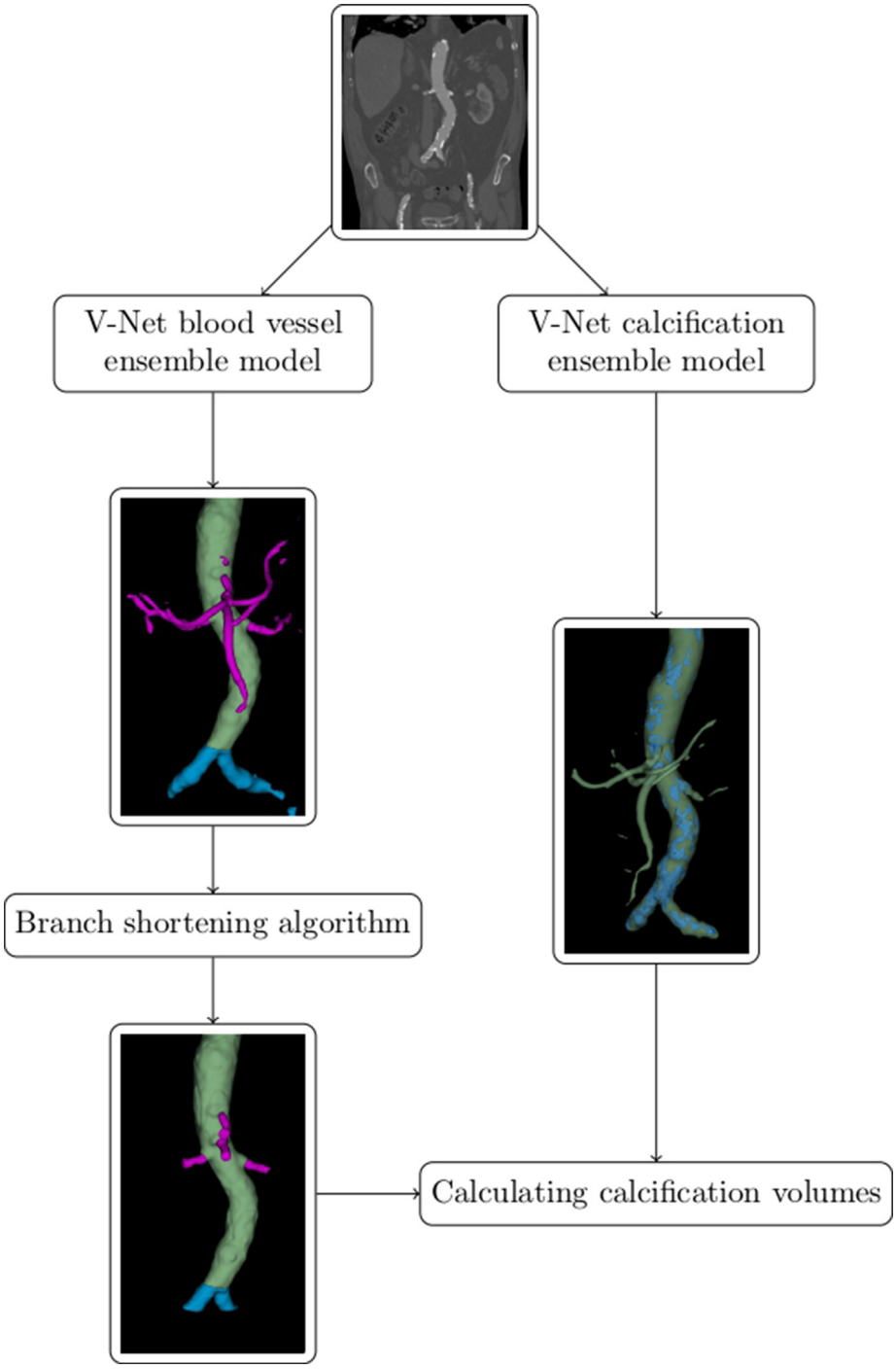

Figure 2 Flow chart of the method for quantifying the calcification of the abdominal aorta and major side branches. The input CT volume is fed to two ensemble V-net models resulting in two segmentations: one of which separates the different arteries and the other one segments the calcification and blood vessels. Artery segmentation is processed by an algorithm that shortens the aortic branches to approximately desired lengths. The calcification volume for each artery is computed by combining the outputs of the algorithm and V-Net calcification ensemble model.

calcifications, the cardiovascular stents were treated as calcifications. The V-Nets of the model were trained for an average of 1,880 epochs. An example prediction of the model is visualised in Fig 2. The calcification volume was calculated from different blood vessels by checking the indexes of the calcifications to those of the blood vessels.

Evaluation metrics

The chosen metrics for the evaluation of the segmentation by the models were the Dice score and volumetric similarity (VS).[26] The evaluation metrics used for the evaluation of the quantity of the calcification in different

arteries were the Pearson correlation coefficient and R-squared (R2) between the ground truth values and the predicted values, which were calculated using Python 3.10.6 modules NumPy v. 1.24.2 and scikit-learn v. 1.2.2, respectively.

The model predicting the blood vessels was evaluated after cutting the veins using the method above. The calcification model was evaluated without any post-processing in order to better evaluate the segmentation of calcifications specifically and only the calcification label was taken into account as the second label was not of interest.

Results

Model results

The ensemble model performance was compared to that of a single model, chosen at random from the ensemble model results are seen in Table 2. Figs 3 and 4 show the comparison between the predictions and ground truths.

Statistical metrics of calcification volume and the effect of vessel segmentation to the metrics

The calcification volume was assessed using the predicted vessels and compared to the volume defined from the ground truth segmentations. Predicted calcification was also assessed based on the ground truth vessel segmentations to evaluate the effect of the automated vessel segmentation on the measured volume. The results are seen in Table 3.

Figs 5–7 visualise the predicted volumes versus the ground truth volumes of the calcification for each patient evaluated using the predicted vessels and the ground truth vessels separately. The impact of stents and prosthetic cases was assessed on the selected evaluation metrics, with the results presented in Tables 3 and 4, demonstrating the influence of stents and prostheses.

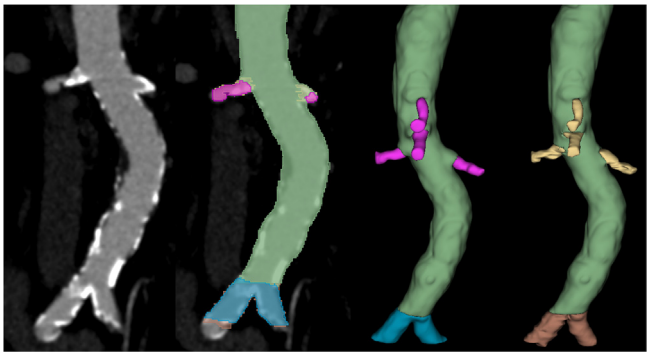

Figure 3 The trimmed vessels. On the left, there is a slice of the CT volume thresholded to emphasize the area of interest. In the next image a slice of the CT volume is shown with arteries labels to illustrate the process. The aorta for both the prediction and the ground truth is shown in green to better illustrate the difference of the segmented base of the aortic branches. 3D rendering of the ground truth processed with branch shortening algorithm is presented as the last image and prediction is presented left of it.

Discussion

The present study describes a novel neural network-based method for automatically quantifying the calcification of the abdominal aorta and its branches to the common iliac arteries, coeliac trunk, renal arteries, and the superior mesenteric artery. The present method uses a convolutional neural network model V-Net that segments calcifications and the aorta and its branches automatically, enabling the quantification of calcification patterns in the aorta and its associated arteries. The method performed had high correlation to the ground truth, especially in the main aorta.

In the study of Summers *et al.*,[27] the authors trained their model partly with contrast-enhanced CT to automatically segment abdominal aortic calcifications and compute the Agatston score based on the segmentations. Unlike in the present study, the calcifications in the aortic branches were not segmented and the precision of the segmentations was not evaluated. During the manual segmentation process, it was discovered that the calcifications could not be segmented accurately with a single threshold in the present dataset. Similar results have been previously reported.[17] Therefore the accuracy of calcification delineations was evaluated via the correlation of the volumes of predicted calcification with the volumes of ground truth calcification. This metric could be used to evaluate both small absolute but large relative differences, and large absolute but small relative differences between volumes. The performance of the V-Net ensembles in the segmentation tasks was measured using the Dice score and volumetric similarity, with a former used as a metric that complemented the Dice score by not considering the overlap of segmented volumes.

Table 2
Ensemble model evaluation metrics and single model evaluation metrics.

Label	Ensemble		Single model	
	Dice score	VS	Dice score	VS
Aorta	0.96 [0.88–0.98]	0.98 [0.92–1]	0.96 [0.87–0.98]	0.99 [0.94–1]
Aortic branches	0.74 [0.29–0.85]	0.87 [0.31–1]	0.71 [0.16–0.86]	0.85 [0.18–0.99]
Common iliac arteries	0.72 [0.21–0.89]	0.91 [0.48–1]	0.71 [0.13–0.91]	0.89 [0.33–1]
Calcification	0.69 [0.42–0.90]	0.80 [0.48–0.98]	0.69 [0.33–0.88]	0.81 [0.44–0.98]

The vessels were predicted by a model then cut using the method above and the metrics of different vessel groups were measured separately. The calcification models were evaluated using the original predictions. The evaluation metrics used were the Dice score and volumetric similarity (VS). The scores were reported to two decimal places for consistency and ease of comparison. The lowest and highest values for the scores were included in brackets.

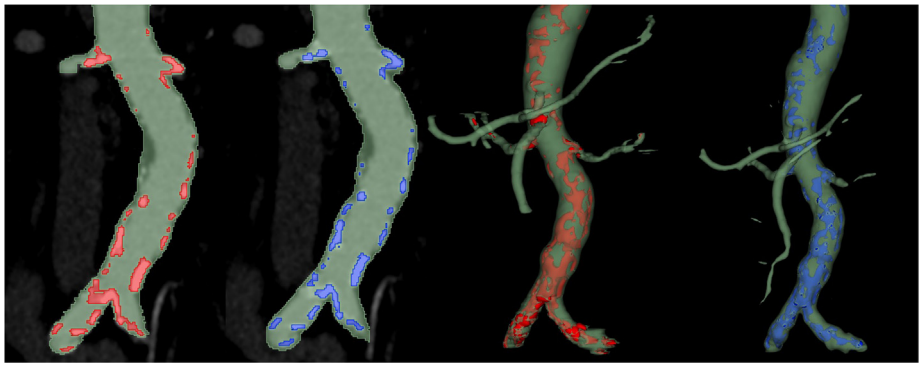

Figure 4 The predicted calcification. The first two images are the prediction and the ground truth segmentations with the ground truth marked as red and the prediction marked as blue. The last two images are the 3D renderings of the ground truth segmentation and the predicted segmentation. The image without any labels is seen in Fig 3.

The segmentation of the aortic branches and common iliac arteries is less accurate than that of the aorta. The results indicate the highest correlation when identifying calcifications in the aorta itself with the lowest correlation for the common iliac arteries when including the stents. The largest discrepancy resulting from blood vessel predictions originated from the branches. This is partly explained by the decision to include the base of the branch in the ground truth into the branch and the model had trouble including the entire base and predicted it at least partly as aorta as can be seen from Fig 3; however, the results show that the evaluation of calcification volume is still of significance even in these arteries and given more training data the model might learn to segment the other arteries more accurately. The correlation was calculated from both the predicted arteries, i.e., using the complete method and from the ground truth arteries in order to better understand the effect of blood vessel segmentation on the correlation between the predicted and ground truth calcification volumes.

Removing the stents from the data did not significantly impact the evaluation metrics for the different models, except that the removal of prosthetic cases affected the prediction scores for the common iliac arteries (Table 4). These changes are noteworthy, considering there was only one prosthetic case in the test set. The correlation coefficient values in Table 3, pertaining to the common iliac arteries, indicate that both prosthetic cases and stents significantly influence the predicted calcification volume and cannot be disregarded in analyses where they are present.

The calcification segmentation included the blood vessels with the intent for the model to better learn the location of the relevant calcifications. The potential impact of vascular stents and prosthetic grafts on the estimated calcification volume can be a limiting factor for the method, as their presence based on the results can affect the accuracy of the calcification segmentation. Table 4 illustrates that the presence of stents changes the correlation with the ground truth significantly and can provide a significantly larger volume of calcification at the location of the stent. The presence of the prosthetic graft affects blood vessel segmentation significantly, as there was limited data for the model to learn that the graft is not part of the blood vessels. Treating the stents as background was considered, but preliminary experiments implied that the number of cases was not enough for the model to learn to distinguish stents from calcifications. The results were not significantly different except for R2 correlation, which, in general, was slightly higher for the model that was trained as stents marked as calcifications with the exception of the calcification predicted from the predicted common iliac arteries (0.17–0.2). It was decided to report on the model that treated them as calcifications during the training.

The ensemble model and the single model cases were compared. Table 2 shows the ensemble model slightly outperformed the single model in the blood vessel segmentation case, mostly by improving the worst results of

Table 3
Statistical evaluation of the models' ability to segment the calcification.

Blood vessel	Pearson correlation	R2	Pearson correlation (no stent)	R2 (no stent)	Pearson correlation (no stent or prothesis)	R2 (no stent or prothesis)
Aorta	0.94 (0.96)	0.85 (0.87)	0.95 (0.96)	0.85 (0.87)	0.97 (0.97)	0.91 (0.91)
Aortic branches	0.84 (0.96)	0.43 (0.85)	0.82 (0.95)	0.36 (0.83)	0.86 (0.97)	0.47 (0.88)
Common iliac arteries	0.60 (0.65)	0.17 (0.38)	0.95 (0.99)	0.90 (0.90)	0.99 (0.99)	0.95 (0.91)

The calcification was evaluated in both the cases of predicted blood vessels fully utilising the method and then separately from the manually segmented ones in both cases the vessels were cut before evaluation. The values for the second case are in brackets and evaluate the effect of the automated blood vessel segmentations on the calcification correlation. The metrics used were the Pearson correlation coefficient and R-squared correlation. Then the metrics were evaluated again while leaving out stent and prosthesis cases. The scores were reported to two decimal places for consistency and ease of comparison.

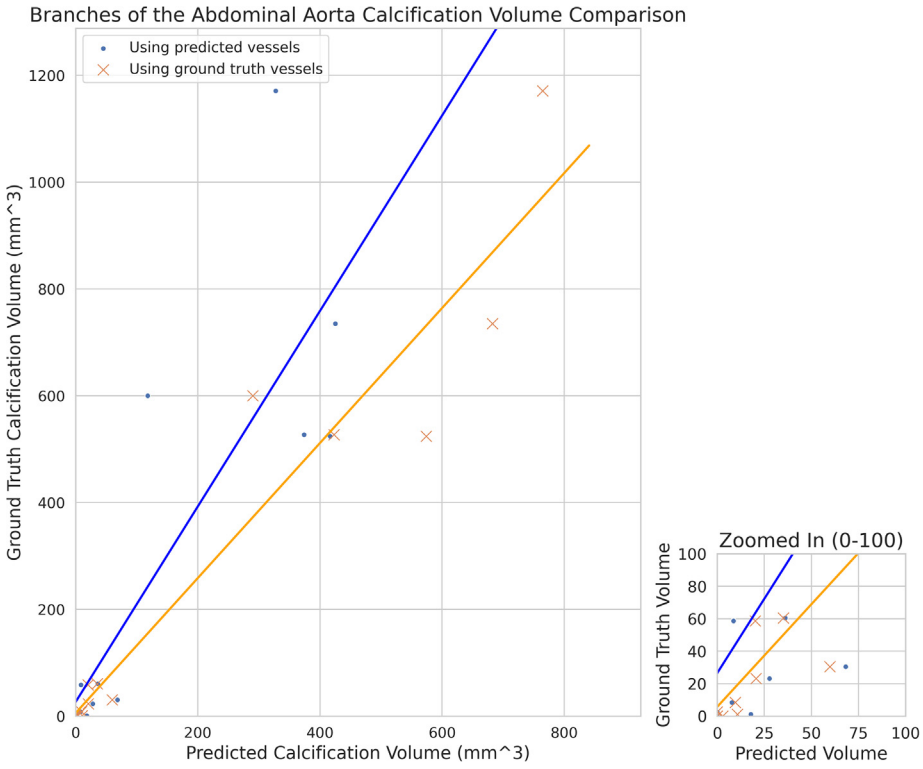

Figure 5 The predicted calcification volume compared with the ground truth one is plotted for the branches. Blue spots refer to predicted volume evaluated using predicted vessels and orange cross refers to predictions evaluated using ground truth vessels. Two lines were fitted through the points blue being the predicted vessels and orange the ground truth vessels. The line was fitted using the least squares method.

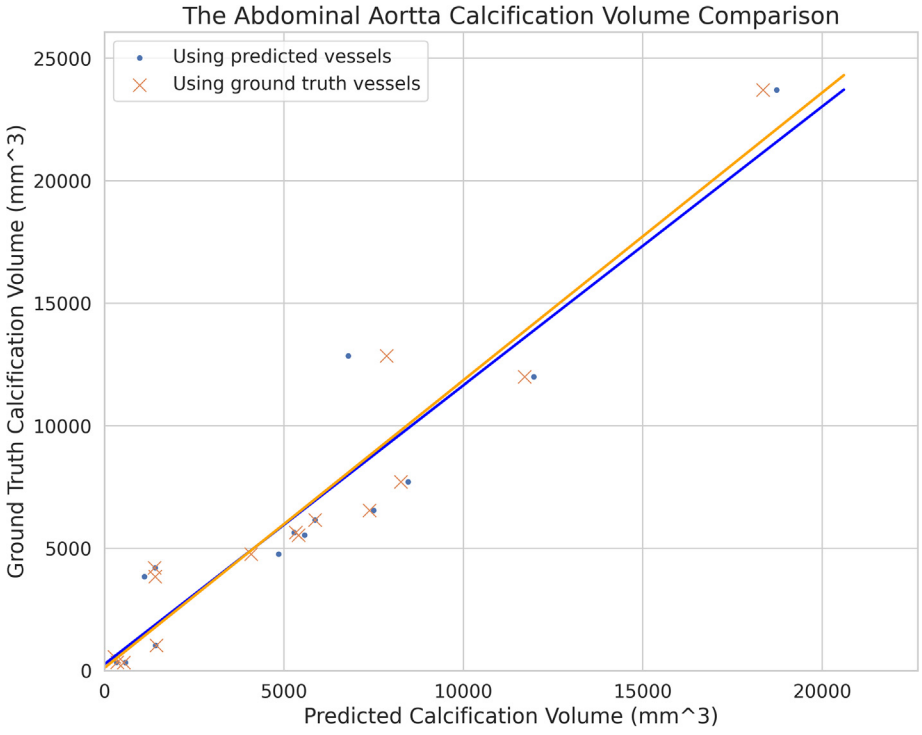

Figure 6 The predicted calcification volume compared with the ground truth one is plotted for the abdominal aorta. Blue spots refer to predicted volume evaluated using predicted vessels and orange cross refers to predictions evaluated using ground truth vessels. Two lines were fitted through the points blue being the predicted vessels and orange being the ground truth vessels. The line was fitted using the least squares method.

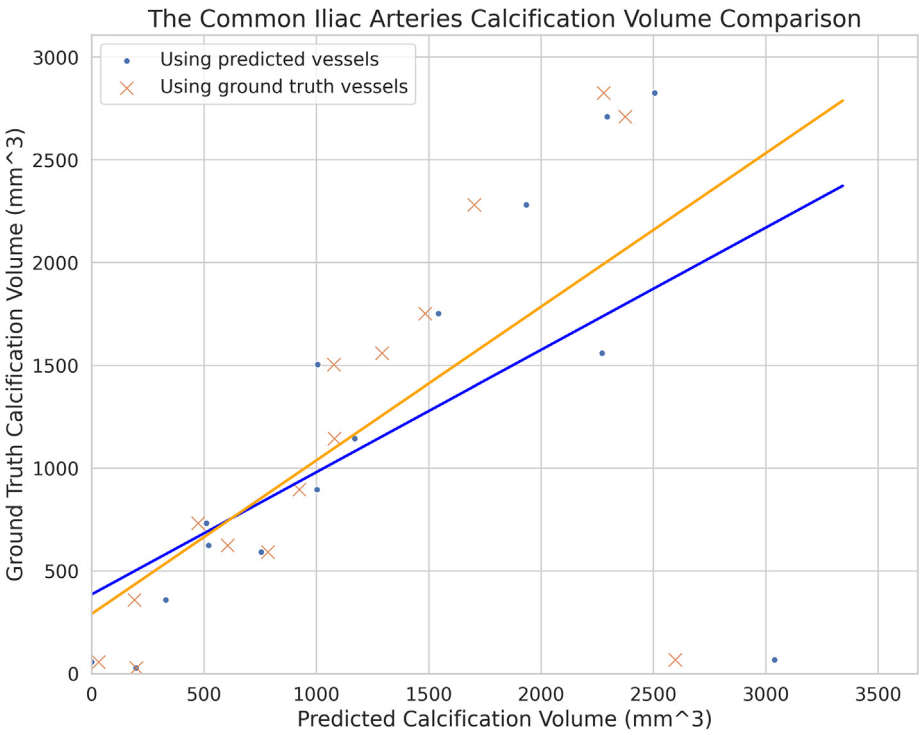

Figure 7 The predicted calcification volume compared with the ground truth one is plotted for the common iliac arteries. Blue spots refer to predicted volume evaluated using predicted vessels and orange cross refers to predictions evaluated using ground truth vessels. Two lines were fitted through the points blue being the predicted vessels and orange the ground truth vessels. The line was fitted using the least squares method.

the single model. In the calcification case, both models performed similarly but the ensemble model had a less wide range of scores.

The present study has its limitations. The ground truths were created by ON. In cases where the annotation was not well-defined, a more experienced radiologist was consulted, especially when the areas were totally occluded or thrombus-filled arteries were difficult to segment. The shortening algorithm has limitations. If the aortic branches run parallel to the aorta and the segmentation of the branch is partially connected to the aorta, it will be mistakenly included from that point as a separate branching point of the aorta and included in the shortened segmentation, as observed in one case in the test set. Another limitation is that the method takes the distance from the closest aorta voxel, which might lead to slightly longer vessels than intended when measuring along the middle line. The choice of training a model that labelled stents as calcifications can also be considered as a deficiency. In the current setting, the present method cannot segment calcifications in the vicinity of the stents correctly. Before the model can be applied to more varied datasets, particularly in patients with peripheral arterial disease, it needs further training with more cases containing stents and prostheses. Despite these limitations and considerations, the present results demonstrated potential for accurate and reliable quantification of aortic calcification in cases where stents were not present. This indicates that the technology has the potential to be a valuable tool in medical imaging, but further research is needed to establish its utility and limitations.

The present method offers several advantages in terms of objective, as it eliminates interobserver variability. Its automated nature allows for the examination of large datasets, which would have been labour-intensive with manual approaches. Additionally, the present method can detect calcification from contrast-enhanced CT images, which is considered the reference standard in aortic

Table 4
Evaluation metrics for the models with stent removed from the collected data along with a different case where prosthesis was also removed.

Label	Dice score (no stent)	VS (no stent)	Dice score (no stent or prothesis)	VS (no stent or prothesis)
Aorta	0.96 [0.88–0.98]	0.98 [0.93–1]	0.97 [0.92–0.98]	0.98 [0.93–1]
Aortic branches	0.73 [0.29–0.86]	0.85 [0.31–1]	0.72 [0.29–0.86]	0.85 [0.31–1]
Common iliac arteries	0.72 [0.21–0.89]	0.91 [0.48–1]	0.75 [0.29–0.89]	0.95 [0.78–1]
Calcification	0.69 [0.42–0.90]	0.79 [0.48–0.98]	0.69 [0.42–0.90]	0.79 [0.48–0.98]

Evaluation metrics used were the Dice score and volumetric similarity (VS). The scores were reported to two decimal places for consistency and ease of comparison. The lowest and highest values were included in brackets.

imaging and is routinely performed on patients with aortic maladies. With further training, the method could provide automatic risk information from routine imaging. Furthermore, it introduces an objective way to monitor disease progression over time, allowing us to track and quantify changes in calcification patterns. Even though cardiovascular risk scores are widely utilised in clinical practice especially in targeting primary prevention, there is uncertainty about their impact on patient outcomes.[28] There are also concerns about the generalisability of risk scores to external populations.[29] Incorporating atherosclerotic calcifications into risk scoring have shown promise in past studies. Coronary artery calcification scoring appears to enhance the precision of risk stratification and aortic calcification has been reported to outperform the Framingham risk score.[30,31] Despite its established associations with increased mortality and morbidity, aortic calcification is not utilised in clinical practice due to the current limitations in scoring feasibility. The existing manual methods for quantifying calcification are not practical for clinical use, necessitating the development of an automated approach applicable to routine imaging to enhance adoption.[2,9,15,16] As there is evidence for renal and visceral artery calcification being independent cardiovascular risk factors, it seems logical to broaden scope to the aortic branches as well.[32–35] The burden of vascular disease and calcification of specific arterial segment in the lower extremity seems to have a significant impact on cardiovascular mortality.[36–39] In future studies it will be interesting to expand the automatic segmentation from the aorta distally to the lower limbs. This would allow comprehensive and reproducible analysis of the overall mortality and cardiovascular risk based on calcification patterns in the arterial system.

Outside overall cardiovascular risk scoring arterial calcification has been associated with increased risk in surgical complications. Aortic and iliac calcifications have shown promise in being a good marker for the risk of anastomotic leakage especially in rectal and oesophageal anastomosis.[8,10,40] Implementing an automated calcification scoring method could aid clinicians in personalising operation plans based on risk.

In conclusion, the present study presents, to the authors' knowledge, the first neural network model capable of automatically segmenting both the aorta and its branches, including calcification, from contrast-enhanced CTA images. This technology shows promise in addressing limitations inherent in earlier methods that relied solely on plain CT images.

The ability to evaluate the aortic branches introduces new opportunities for research within the field of atherosclerosis and extends to other areas such as nephrology and gastroenterology. This potentiality broadens the investigative scope, paving the way for diverse and multidisciplinary inquiries.

Conflict of interest

The authors declare no conflict of interest.

Acknowledgments

This study received funding from HUS Diagnostic Center, Helsinki University Hospital (SS: Y780023032). Along with Federal Grant Satasairaala and Kulttuurisäätiö Satakunnan rahasto grant number: 75212239 and 75221501.

References

1. Institute for Health Metrics and Evaluation (IHME). *Global burden of disease collaborative network*. 2019. Global Burden of Disease Study (GBD 2019). Results, https://vizhub.healthdata.org/gbd-results/ [Accessed 12 December 2023].
2. Rantasalo V, Laukka D, Nikulainen V, *et al*. Aortic calcification index predicts mortality and cardiovascular events in operatively treated patients with peripheral artery disease: a prospective PURE ASO cohort follow-up study. *J Vasc Surg* 2022;**76**(6):1657–1666.e2. https://doi.org/10.1016/j.jvs.2022.07.001.
3. Mäkelä S, Asola M, Hadimeri H, *et al*. Abdominal aortic calcifications predict survival in peritoneal dialysis patients. *Perit Dial Int* 2018;**38**(5):366–73. https://doi.org/10.3747/pdi.2017.00043.
4. Hanada S, Ando R, Naito S, *et al*. Assessment and significance of abdominal aortic calcification in chronic kidney disease. *Nephrol Dial Transplant* 2010;**25**(6):1888–95. https://doi.org/10.1093/ndt/gfp728.
5. Kuller LH, Matthews KA, Sutton-Tyrrell K, *et al*. Coronary and aortic calcification among women 8 years after menopause and their premenopausal risk factors: the Healthy Women Study. *Arterioscler Thromb Vasc Biol* 1999;**19**(9):2189–98. https://doi.org/10.1161/01.ATV.19.9.2189.
6. Nielsen M, Ganz M, Lauze F, *et al*. Distribution, size, shape, growth potential and extent of abdominal aortic calcified deposits predict mortality in postmenopausal women. *BMC Cardiovasc Disord* 2010;**10**(1):56. https://doi.org/10.1186/1471-2261-10-56.
7. Parr A, Buttner P, Shahzad A, *et al*. Relation of infra-renal abdominal aortic calcific deposits and cardiovascular events in patients with peripheral artery disease. *Am J Cardiol* 2010;**105**(6):895–9. https://doi.org/10.1016/j.amjcard.2009.10.067.
8. Knight KA, Horgan PG, McMillan DC, *et al*. The relationship between aortic calcification and anastomotic leak following gastrointestinal resection: a systematic review. *Int J Surg* 2020;**73**:42–9. https://doi.org/10.1016/j.ijsu.2019.11.023.
9. Ohya M, Otani H, Kimura K, *et al*. Vascular calcification estimated by aortic calcification area index is a significant predictive parameter of cardiovascular mortality in hemodialysis patients. *Clin Exp Nephrol* 2011;**15**(6):877–83. https://doi.org/10.1007/s10157-011-0517-y.
10. Goense L, van Rossum PSN, Weijs TJ, *et al*. Aortic calcification increases the risk of anastomotic leakage after Ivor–Lewis esophagectomy. *Ann Thorac Surg* 2016;**102**(1):247–52. https://doi.org/10.1016/j.athoracsur.2016.01.093.
11. Goff DC, Lloyd-Jones DM, Bennett G, *et al*. 2013 ACC/AHA guideline on the assessment of cardiovascular risk: a report of the American College of Cardiology/American heart association task force on practice guidelines. *Circulation* 2014;**129**(Suppl. 2), https://doi.org/10.1161/01.cir.0000437741.48606.98.
12. Piepoli MF, Hoes AW, Agewall S, *et al*. 2016 European guidelines on cardiovascular disease prevention in clinical practice. *Atherosclerosis* 2016;**252**:207–74. https://doi.org/10.1016/j.atherosclerosis.2016.05.037.
13. Collins GS, Altman DG. An independent and external validation of QRISK2 cardiovascular disease risk score: a prospective open cohort study. *BMJ* 2010;**340**:c2442. https://doi.org/10.1136/bmj.c2442. c2442.
14. Bitton A, Gaziano T. The Framingham Heart Study's impact on global risk assessment. *Progr Cardiovasc Dis* 2010;**53**(1):68–78. https://doi.org/10.1016/j.pcad.2010.04.001.
15. Taniwaki H, Ishimura E, Tabata T, *et al*. Aortic calcification in haemodialysis patients with diabetes mellitus. *Nephrol Dial Transplant* 2005;**20**(11):2472–8. https://doi.org/10.1093/ndt/gfi039.
16. Kauppila LI, Polak JF, Cupples LA, *et al*. New indices to classify location, severity and progression of calcific lesions in the abdominal aorta: a 25-year follow-up study. *Atherosclerosis* 1997;**132**(2):245–50. https://doi.org/10.1016/S0021-9150(97)00106-8.

17. Holcombe SA, Horbal SR, Ross BE, *et al*. Variation in aorta attenuation in contrast-enhanced CT and its implications for calcification thresholds. *PLoS One* 2022;**17**(11):e0277111, https://doi.org/10.1371/journal.pone.0277111.
18. Reid S, Schousboe JT, Kimelman D, *et al*. Machine learning for automated abdominal aortic calcification scoring of DXA vertebral fracture assessment images: a pilot study. *Bone* 2021;**148**:115943, https://doi.org/10.1016/j.bone.2021.115943.
19. Graffy PM, Liu J, O'Connor S, *et al*. Automated segmentation and quantification of aortic calcification at abdominal CT: application of a deep learning-based algorithm to a longitudinal screening cohort. *Abdom Radiol* 2019;**44**(8):2921–8. https://doi.org/10.1007/s00261-019-02014-2.
20. Jolesz FA, editor. *Intraoperative imaging and image-guided therapy*. New York: Springer; 2014.
21. Kesävuori R, Kaseva T, Salli E, *et al*. Deep learning-aided extraction of outer aortic surface from CT angiography scans of patients with Stanford type B aortic dissection. *Eur Radiol Exp* 2023;**7**:35.
22. Milletari F, Navab N, Ahmadi S-A. *V-Net: Fully convolutional neural networks for volumetric medical image segmentation*, **1606**; 2016:04797, https://doi.org/10.48550/arXiv.1606.04797. arXiv.
23. The Monai Consortium. *Project MONAI Zenodo* 2020, https://doi.org/10.5281/ZENODO.4323059.
24. Lowekamp BC, Chen DT, Ibáñez L, *et al*. The design of SimpleITK. *Front Neuroinform* 2013;**7**, https://doi.org/10.3389/fninf.2013.00045.
25. Vincent L. Morphological transformations of binary images with arbitrary structuring elements. *Signal Process* 1991;**22**(1):3–23. https://doi.org/10.1016/0165-1684(91)90025-E.
26. Taha AA, Hanbury A. Metrics for evaluating 3D medical image segmentation: analysis, selection, and tool. *BMC Med Imaging* 2015;**15**(1):29. https://doi.org/10.1186/s12880-015-0068-x.
27. Summers RM, Elton DC, Lee S, *et al*. Atherosclerotic plaque burden on abdominal CT: automated assessment with deep learning on non-contrast and contrast-enhanced scans. *Acad Radiol* 2021;**28**(11):1491–9. https://doi.org/10.1016/j.acra.2020.08.022.
28. Collins DRJ, Tompson AC, Onakpoya IJ, *et al*. Global cardiovascular risk assessment in the primary prevention of cardiovascular disease in adults: systematic review of systematic reviews. *BMJ Open* 2017;**7**(3):e013650, https://doi.org/10.1136/bmjopen-2016-013650.
29. Sofogianni A, Stalikas N, Antza C, *et al*. Cardiovascular risk prediction models and scores in the era of personalized medicine. *J Pers Med* 2022;**12**(7):1180. https://doi.org/10.3390/jpm12071180.
30. Peters SAE, Den Ruijter HM, Bots ML, *et al*. Improvements in risk stratification for the occurrence of cardiovascular disease by imaging subclinical atherosclerosis: a systematic review. *Heart* 2012;**98**(3):177–84. https://doi.org/10.1136/heartjnl-2011-300747.
31. O'Connor SD, Graffy PM, Zea R, *et al*. Does nonenhanced CT-based quantification of abdominal aortic calcification outperform the Framingham risk score in predicting cardiovascular events in asymptomatic adults? *Radiology* 2019;**290**(1):108–15. https://doi.org/10.1148/radiol.2018180562.
32. Roseman DA, Hwang S-J, Manders ES, *et al*. Renal artery calcium, cardiovascular risk factors, and indexes of renal function. *Am J Cardiol* 2014;**113**(1):156–61. https://doi.org/10.1016/j.amjcard.2013.09.036.
33. Lin TC, Wright CM, Criqui MH, *et al*. Superior mesenteric artery calcification is associated with cardiovascular risk factors, systemic calcified atherosclerosis, and increased mortality. *J Vasc Surg* 2018;**67**(5):1484–90. https://doi.org/10.1016/j.jvs.2017.08.081.
34. Thomas IC, Ratigan AR, Rifkin DE, *et al*. The association of renal artery calcification with hypertension in community-living individuals: the multiethnic study of atherosclerosis. *J Am Soc Hypertens* 2016;**10**(2):167–74. https://doi.org/10.1016/j.jash.2015.12.003.
35. Miura S, Kurimoto Y, Iba Y, *et al*. Quantitative evaluation of superior mesenteric artery calcification in hemodialysis patients undergoing aortic valve replacement. *Gen Thorac Cardiovasc Surg* 2020;**68**(11):1252–9. https://doi.org/10.1007/s11748-020-01352-z.
36. Wickström J-E, Virtanen J, Aro E, *et al*. Bilateral low systolic toe pressure and toe-brachial index are associated with long-term mortality in patients with peripheral artery disease. *J Vasc Surg* 2019;**70**(6):1994–2004. https://doi.org/10.1016/j.jvs.2019.03.073.
37. Wickström J-E, Jalkanen JM, Venermo M, *et al*. Crural Index and extensive atherosclerosis of crural vessels are associated with long-term cardiovascular mortality in patients with symptomatic peripheral artery disease. *Atherosclerosis* 2017;**264**:44–50. https://doi.org/10.1016/j.atherosclerosis.2017.07.023.
38. Wickström J-E, Virtanen J, Laivuori M, *et al*. Data on association of ankle pressure and ankle brachial index of symptomatic and contralateral lower extremities with overall and cardiovascular mortality in patients with lower extremity peripheral artery disease. *Data Brief* 2018;**20**:691–7. https://doi.org/10.1016/j.dib.2018.08.041.
39. Jalkanen JM, Wickström J-E, Venermo M, *et al*. The extent of atherosclerotic lesions in crural arteries predicts survival of patients with lower limb peripheral artery disease: a new classification of crural atherosclerosis. *Atherosclerosis* 2016;**251**:328–33. https://doi.org/10.1016/j.atherosclerosis.2016.04.016.
40. Pochhammer J, Tröster F, Blumenstock G, *et al*. Calcification of the iliac arteries: a marker for leakage risk in rectal anastomosis—a blinded clinical trial. *Int J Colorectal Dis* 2018;**33**(2):163–70. https://doi.org/10.1007/s00384-017-2949-7.